Bio-Design and Manufacturing (2022) 5:265–276
https://doi.org/10.1007/s42242-021-00178-9

RESEARCH ARTICLE

Development of a 3D subcutaneous construct containing insulin-producing beta cells using bioprinting

Chi B. Ahn[1] · Ji-Hyun Lee[1] · Joo H. Kim[2] · Tae H. Kim[2] · Hee-Sook Jun[3] · Kuk H. Son[4] · Jin W. Lee[1,2]

Received: 6 June 2021 / Accepted: 23 November 2021 / Published online: 25 January 2022

Abstract

Type 1 diabetes is caused by insulin deficiency due to the loss of beta cells in the islets of Langerhans. In severe cases, islet transplantation into the portal vein is performed. However, due to the loss of transplanted islets and the failure of islet function, the 5-year insulin independence rate of these patients is < 50%. In this study, we developed a long-term, insulin-secreting, 3D-bioprinted construct implanted subcutaneously with the aim of preventing islet loss. The bioprinted construct was fabricated by the multi-layer bioprinting of beta-cell (mouse insulinoma-6: MIN-6)-encapsulated alginate bioink and poly(caprolactone) biodegradable polymer. A glucose response assay revealed that the bioprinted constructs proliferated and released insulin normally during the 4-week in vitro period. Bioprinted MIN-6 generated clusters with a diameter of 100–200 μm, similar to the original pancreatic islets in the construct. In an in vivo study using type 1 diabetes mice, animals implanted with bioprinted constructs showed three times higher insulin secretion and controlled glucose levels at 8 weeks after implantation. Because the implanted, bioprinted constructs had a positive effect on insulin secretion in the experimental animals, the survival rate of the implanted group (75%) was three times higher than that of the non-implanted group (25%). The results suggest that the proposed, 3D-bioprinted, subcutaneous construct can be a better alternative to portal vein islet transplantation.

Chi B. Ahn and Ji-Hyun Lee have contributed equally to this work.

✉ Kuk H. Son
dr632@gilhospital.com

✉ Jin W. Lee
jwlee@gachon.ac.kr

[1] Department of Molecular Medicine, College of Medicine, Gachon University, 155, Gaetbeol-ro, Yeonsu-ku, Incheon, Republic of Korea

[2] Department of Health Sciences and Technology, GAIHST, Gachon University, 155, Gaetbeol-ro, Yeonsu-ku, Incheon, Republic of Korea

[3] College of Pharmacy, Gachon University, 191, Hambangmoe-ro, Yeonsu-ku, Incheon, Republic of Korea

[4] Department Thoracic and Cardiovascular Surgery, Gachon University Gil Medical Center, College of Medicine, Gachon University, 21, Namdong-daero 774 beon-gil, Namdong-gu, Incheon, Republic of Korea

Graphic abstract

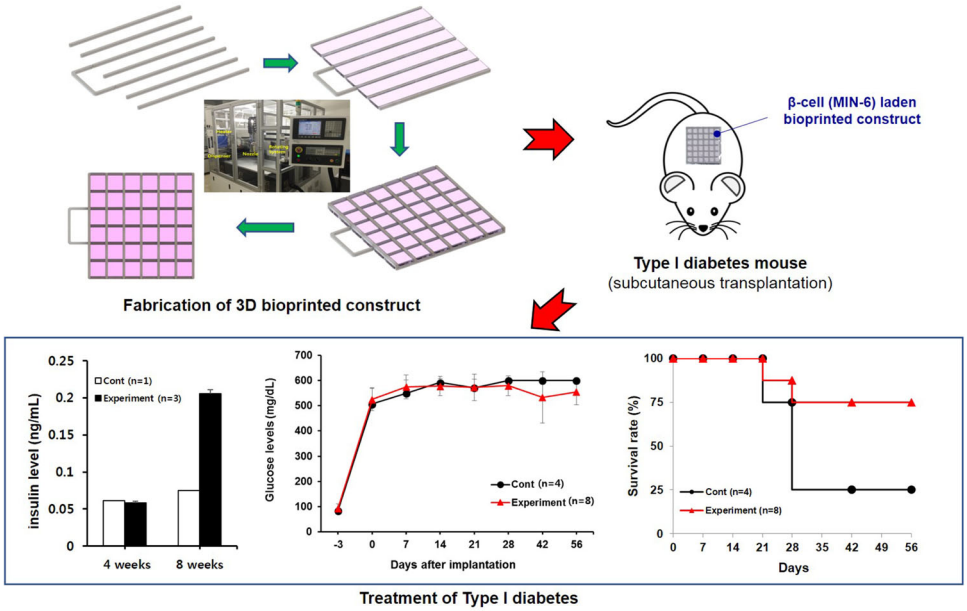

Keywords 3D bioprinting · Subcutaneous construct · Type 1 diabetes · Insulin · Beta cells

Introduction

Diabetes, characterized by a loss of glycemic control, affects more than 400 million people worldwide [1, 2]. Importantly, in 2017, approximately 4 million people between the ages of 20 and 79 years died due to health complications resulting from diabetes, which is 10.7% of global mortality [3]. Furthermore, the rapid increase in the number of obese people has led to a sharp increase in the risk of diabetes in developed countries, including in the USA. Diabetes is considered a serious disease that needs to be addressed with a sense of urgency worldwide.

Diabetes results from the malfunction of the beta cells present in the islets of Langerhans in the pancreas due to either an autoimmune-mediated disorder (type 1) or insulin resistance in the peripheral tissues (type 2). Diabetes management is based on diet (type 1 and 2) and exercise therapy (type 2), and drug therapy is initiated if blood glucose is not controlled through the former methods. Depending on the state of glycemic control, the use of an oral hypoglycemic agent (type 2), glucagon-like peptide-1 receptor agonist (type 2) or an insulin treatment (types 1 and 2) is considered. Insulin is administered either by daily injections or by an insulin pump that delivers a continuous insulin infusion. However, when blood glucose control using insulin injection is difficult because of recurrent severe hyperglycemia, a surgical treatment is the only solution, and donor islets or pancreas are transplanted. Most pancreatic islet transplants are performed via the portal vein, and many initial immune rejection reactions are observed after transplantation. The 5-year independence rate of patients has been reported to be less than 50% after transplantation [4, 5].

There are several reasons for the low survival rate of islet transplants. First, there is an instant inflammatory reaction induced by complement activation and the innate immune response [5]. Second, destruction of cell-extracellular matrix interaction occurs during cell isolation from the donor's pancreas. Third, islet vasculature for nutrition and oxygen supply is damaged after transplantation [6–10]. Fourth, islets are injured by drugs and toxins produced by the liver [11, 12]. Other causes are the immune response and recurrent autoimmunity [4]. Furthermore, the long-term survival of the transplanted islets seems to be difficult owing to a combination of these factors.

As a solution to the low survival and functional rate of islet transplantation, the transplantation in non-pancreatic locations, including the kidney capsule [13–15], fat pad [16], subcutaneous sites [17–19], intraperitoneal cavity [20, 21], and the omentum [22], has been investigated. In particular, extrahepatic transplantation of tissue-engineered constructs using a scaffold, which is an environment that protects the islets, has been attracting attention. For several decades, the porous scaffold fabrication using various biomaterials, such as poly(DL-lactide-co-glycolide) acid (PLGA) [23–25],

PLGA scaffolds [26], polydimethylsiloxane salt-leached scaffolds [22, 27], and thermoformed microwell scaffolds of poly(ethylene oxide terephthalate)–poly(butylene terephthalate) (PEOT/PBT) block copolymer [28], has been studied for extrahepatic islet entrapment and transplantation. However, it is difficult to scale up these tissue-engineered constructs to a clinically relevant size due to limitations in the supply of nutrients and oxygen.

Another method of Langerhans islet protection is their encapsulation in hydrogels. In this case, beta cells embedded in small alginate beads or mixed in bulk alginate hydrogels are injected into the abdominal cavity or subcutaneously [29, 30]. Ludwig et al. reported the creation of an oxygenated, immunoprotective, alginate-based, macro-chamber for beta-cell transplantation in male patients. However, the requirement of attaching an external large module for oxygen supply is a major drawback of this strategy [31].

Recently, attempts have been made to use 3D printing in regenerative medicine. 3D printing is a technology that produces 3D objects by converting complex 3D shapes into digital data and stacking. In particular, 3D printing has the advantage of producing patient-customized constructs by combining medical image data, including computed tomography and magnetic resonance imaging, with reverse-engineering technology. Furthermore, as a branch of 3D printing, 3D-bioprinting technology, which mounts cells and growth factors in bioinks and prints them simultaneously with structural biomaterials, presents new possibilities for the reconstruction of soft and complex tissues.

To date, 3D printing and 3D-bioprinting technology have been used to reconstruct human organs, such as the ears, nose, trachea, bone, cartilage, skin, liver tissue, and myocardial tissues, and their areas of application are expanding [32–41]. Recently, there have also been attempts to use 3D printing for the treatment of diabetes. It was used to form a cage containing beta cells [4] or to produce a two-dimensional structure [42, 43]. If 3D-bioprinting technology can create a 3D structure similar to human tissue using beta-cell bioink, it may help to improve the survival and function of islet cells. In addition, by optimizing the composition of the bioink, it is expected to solve the problem of mere islet transplantation or subcutaneous implant patches.

In this study, we propose an insulin-secreting construct using 3D-bioprinting technology that works normally for a long time by expanding into large cell aggregates with a diameter of 100–200 μm in vitro and is easily implanted subcutaneously. After transplanting the developed structure into type 1 diabetes mice, the possibility of the functional replacement of a damaged pancreas was verified by evaluating insulin secretion and the survival rate. Our results demonstrate new possibilities for 3D bioprinting for the treatment of diabetes.

Materials and methods

Mouse beta-cell (MIN-6) culture

Mouse insulinoma-6 cells (MIN-6) were cultured in Dulbecco's modified Eagle's medium (DMEM; Gibco, Waltham, MA, USA) containing 10% fetal bovine serum (FBS; Gibco, Waltham, MA, USA) and 100 units/mL of penicillin/streptomycin (P/S; Gibco) at 37 °C in a humidified, 5% CO_2 atmosphere. When the cells reached confluence, they were removed from the culture dish using 0.25% trypsin–ethylenediaminetetraacetic acid (EDTA; Gibco), centrifuged, and resuspended in DMEM. The medium was exchanged every two days. For the bioprinting and cell tests, MIN-6 of passage number from 20 to 24 was used.

Preparation of alginate mixtures and cells encapsulated within bulk hydrogels

The alginate solution was prepared from low-viscosity sodium alginate (Sigma, St. Louis, MO, USA) and DMEM with 10% FBS. The MIN-6 suspension, at a density of 2×10^5 cells, was added to the alginate solution at concentrations of 1, 2, 3, and 4%. Calcium chloride (Sigma) dissolved in deionized water at a concentration of 100 mM was added to the well to cross-link the alginate and form a hydrogel. Half an hour later, the cross-linked hydrogels were washed three times, submerged in DMEM, and then incubated at 37 °C in a humidified, 5% CO_2 environment. The cell medium was exchanged every two days.

3D-bioprinting system for the fabrication of the cell-laden subcutaneous construct

3D constructs were fabricated using a multi-head, deposition-based 3D-printing system (Geo technology, Incheon, Korea). This system is equipped with controller for x–y–z motion, temperature, and pneumatic (Musashi Engineering Inc, Tokyo, Japan). Two isolated heads assembled with a heater and syringe enabled the fabrication of hybrid constructs with various combinations of biomaterials. The pressure and temperature of each head were individually controlled to 800 kPa and 300 °C, respectively. A linear motor, linear encoder, and linear guide were installed to control the x- and y-axis motions with an accuracy of 0.5 μm and repeatability of 2 μm. To control the z-axis, ball-screw motors with encoders were installed. The accuracy and repeatability of the z-axis were both 5 μm. The maximum product size of this system was 400 × 400 × 250 mm.

Fabrication of 3D-bioprinted constructs

3D-bioprinted constructs were fabricated using the developed 3D-printing system. In brief, the biodegradable polymers in the syringe, PCL, and MIN-6-laden alginate bioink were printed to the specified location by operation codes from a computer-aided design (CAD) file, and the printed alginate hydrogels were hardened using a calcium chloride solution. After printing a single layer, the printer head moved to the next position and printed the PCL frame and alginate bioink. Using the layer-by-layer process, we fabricated a 3D construct. The printing conditions for the PCL strut were as follows: a printing speed of 200 mm/min, an air pressure of 600 kPa, and a syringe temperature of 65 °C. The printing conditions for the MIN-6-encapsulated, alginate bioink were as follows: a printing speed of 50 mm/min, an air pressure of 150 kPa, and a syringe temperature of 22 °C.

Cell viability assays

MIN-6 cell-encapsulated scaffolds with a density of 2×10^5 cells/alginate scaffold were cultured in a 24-well plate for 28 days. To assess cell survival, a live/dead fluorescent solution of calcein-acetoxymethyl (AM) and ethidium homodimer-1 (EthD-1) was prepared according to the manufacturer's instructions (Thermo Fisher, Waltham, MA, USA). Then, the scaffolds were submerged in the solution and incubated at 37 °C for 40 min, before being washed in phosphate-buffered saline (PBS; Gibco). After being washed, the scaffolds were observed under a fluorescence microscope (Zeiss LSM 510, Oberkochen, Germany).

Cell proliferation assays

Cell proliferation rates were measured using a cell-counting kit (CCK-8; Dojindo, Kumamoto, Japan). MIN-6 cell-encapsulated scaffolds with a density of 2×10^5 cells/alginate scaffold were cultured in a 24-well plate. After 7, 14, 21, and 28 days, 250 μL of CCK-8 solution was added to each well, and the plate was incubated at 37 °C for 2 h. After extracting the reacted solution from the well plate, the absorbance was measured at 450 nm using an enzyme-linked immunosorbent assay (ELISA) reader (VERSAmax, CA, USA).

In vitro glucose-stimulated insulin secretion

The density of MIN-6 was adjusted to 2×10^5 cells/mL. MIN-6, cell-encapsulated scaffolds with a density of 2×10^5 cells/alginate scaffold were cultured in a 24-well plate, and the scaffolds were divided into low-glucose (LG) and high-glucose (HG) groups. In the MIN-6 culture period of 28 days, the LG and HG groups were adjusted by adding DMEM containing 3.0 and 33.0 glucose, respectively [44, 45]. Insulin production from the cell supernatants was measured using a mouse insulin ELISA kit (ALPCO, Salem, NH, USA).

Animal model and transplantation

Eight-week-old, male ICR mice weighing 30 g (Orientbio, Gyeonggi-do, Korea) were used to induce type 1 diabetes and were kept under controlled specific pathogen free (SPF) conditions (22–24 °C, 55–60% room humidity) under a 12-h light/dark cycle. During the experimental period, the mice were allowed free access to water and a standard rodent diet and were acclimated for 1 week. The study protocol was approved by the Animal Subjects Committee of Gachon University (Approval number: LCDI-2018-0057). After overnight fasting (the mice were deprived of food for 16 h but allowed free access to water), the mice were injected intraperitoneally with freshly prepared streptozotocin (STZ; 180 mg/kg body weight, Sigma Chemical Co., St. Louis, MO, USA) in 0.1 M citrate buffer (pH 4.5). After 3 days, mice with marked hyperglycemia (fasting blood glucose > 300 mg/dL) were considered to have moderate diabetes and were used for the animal study. A bioprinting alginate scaffold containing 2×10^5 MIN-6 cells was implanted into a subcutaneous pocket in the dorsum of each mouse. In the experimental group, a total of eight scaffolds were transplanted into diabetes-induced mice. In the control group, alginate scaffolds without cells were transplanted into diabetes-induced mice ($n = 4$). The animals were sacrificed on days 28 and 56.

In vivo measurement of insulin secretion by glucose stimulation

Once every week, blood samples were drawn from the lateral tail vein between 09:00 AM and 11:00 AM to measure blood glucose levels. Glucose concentrations were determined using an Accu-Check Advantage Blood Glucose Monitor (Roche Group, Mannheim, Germany). Plasma insulin levels (ng/mL) were measured using a mouse insulin ELISA kit (ALPCO, Salem, NH, USA).

Histological assay

Extracted mouse subcutaneous grafts were fixed in 4% paraformaldehyde (PFA; Bioworld, Gyeonggi-do, Korea), embedded in paraffin, and sectioned to a thickness of 4 μm. For hematoxylin and eosin staining, slices were placed, after deparaffinization, in hematoxylin (Sigma, St. Louis, MO, USA) for 5 min, washed with deionized water(DI) water, and dipped into 1% acid alcohol (HCl + 70% EtOH) for 10 s. After washing with DI water, the slices were dipped in eosin (Sigma, St. Louis, MO, USA) for 3 min, washed with DI

water, and then dipped into ammonia for 10 s. Subsequently, they were washed with DI water and dehydrated using 70, 80, 90, and 100% ethanol (Sigma, St. Louis, MO, USA) and xylene (Sigma, St. Louis, MO, USA). For immunohistochemistry, the sections were deparaffinized and dehydrated using xylene and ethanol in series. A staining was performed using a peroxidase immunohistochemistry (IHC) detection kit (Thermo Fisher, Waltham, MA, USA), insulin antibody (Abcam, Cambridge, UK), and CD31 antibody (Santa cruz, Dallas, USA) of a dilution of 1:100. After being washed, the sections were treated with biotinylated anti-rabbit antibody (diluted at 1:200; Abcam) and anti-goat antibody (diluted at 1:500; Abcam) and were then incubated in streptavidin conjugated with peroxidase. The staining was detected using 3, 3-diaminobenzidine (DAB), and all images were captured at a magnification of 5×. Analysis was done by using the core facility center for cell to in vivo (Bio) imaging of Gachon University.

Statistical analysis

All experiments were repeated three times, and the average values are presented unless otherwise stated. Data are presented as mean ± standard deviation. A single-factor analysis of variance with Tukey's multiple comparison test was performed to determine statistical significance ($^{*}P < 0.05$, $^{**}P < 0.01$, $^{***}P < 0.001$).

Results

Fabrication results of the 3D-bioprinted construct

The constructs were printed using a multi-head, deposition-based, 3D-printing system (Fig. 1). The poly(caprolactone) (PCL) polymer frame and MIN-6 encapsulated alginate bioink were successfully printed to the specified location using operation codes (Supplementary Data 1). PCL struts with a diameter of 300 μm were fabricated using a stainless-steel nozzle with a diameter of 300 μm at a printing speed of 200 mm/min, air pressure of 600 kPa, and a syringe temperature of 65 °C. MIN-6-encapsulated alginate bioink struts were printed using an 800 μm diameter, plastic nozzle at a printing speed of 50 mm/min, air pressure of 150 kPa, and a syringe temperature of 22 °C. In addition, we incorporated a forceps handler into the construct for ease of handling. The 3D construct was 10 × 8 mm wide and 0.6 mm thick. Figure 1 shows the control and experimental samples printed using the proposed system.

Optimization of hydrogel concentration for beta-cell proliferation

To set the optimal concentration of hydrogel for the fabrication of a 3D-bioprinted construct, a cell culture was performed by the encapsulation of MIN-6 in alginate at 1, 2, 3, and 4% concentrations. As shown in the live/dead images, the construct at 1% concentration had few cells after 7 days, and at 2% concentration, the number of cells increased slightly on day 7 compared to day 1 (Figs. 2a and 2b). Cell growth was noticeable at concentrations of 3 and 4%. The lower light intensities of samples with concentrations of 1 and 2% were due to the loss of cells caused by the decomposition of the alginate hydrogel during the experiment time of 7 days. However, cell viabilities were maintained above 85% at all alginate concentrations, regardless of the incubation time (Fig. 2c).

To observe these decomposition phenomena in more detail, hydrogel beads were prepared, and the decomposition status over time was examined. At 1% concentration, most of the hydrogel beads were decomposed on day 7, and most of the beta cells inside the hydrogel flowed out. At 2% concentration, on day 7 the hydrogel beads were cracked and divided, and only dead cells increased without increasing the total number of cells. From day 10, the bead at 3% concentration did not maintain the bead structure due to swelling by hydration, and the hydrogel bead became transparent over time. However, the alginate beads at 4% concentration retained their spherical shape for 10 days (Fig. 3). When we observed the degradation of alginate over a period of time, we confirmed that 4% alginate maintained the bead structure for more than 30 days in phosphate-buffered saline. It was confirmed that a 4% alginate concentration is required for long-term cell culture.

Based on the above results, constructs that were fabricated using 4% alginate were cultured in vitro for 4 weeks. At the live/dead assay result, the number of beta cells continuously increased over the entire period (Fig. 4a). During the entire culture period of 28 days, the bioprinted constructs maintained a cell viability of more than 85% (Fig. 4b). In particular, from day 21, we confirmed that the cell-laden hydrogel constructs extended to large cell aggregates of 100–200 μm in diameter, such as pseudo-islet structures. The quantitative evaluation of cell proliferation using CCK-8 also confirmed the increase in beta-cell populations over time (Fig. 5).

Insulin secretion from the 3D-bioprinted construct

Although the growth of beta cells inside the fabricated construct is important, their normal function is more important. To this end, insulin secretion for glucose stimulation in MIN-6 cells encapsulated in alginate was observed using an

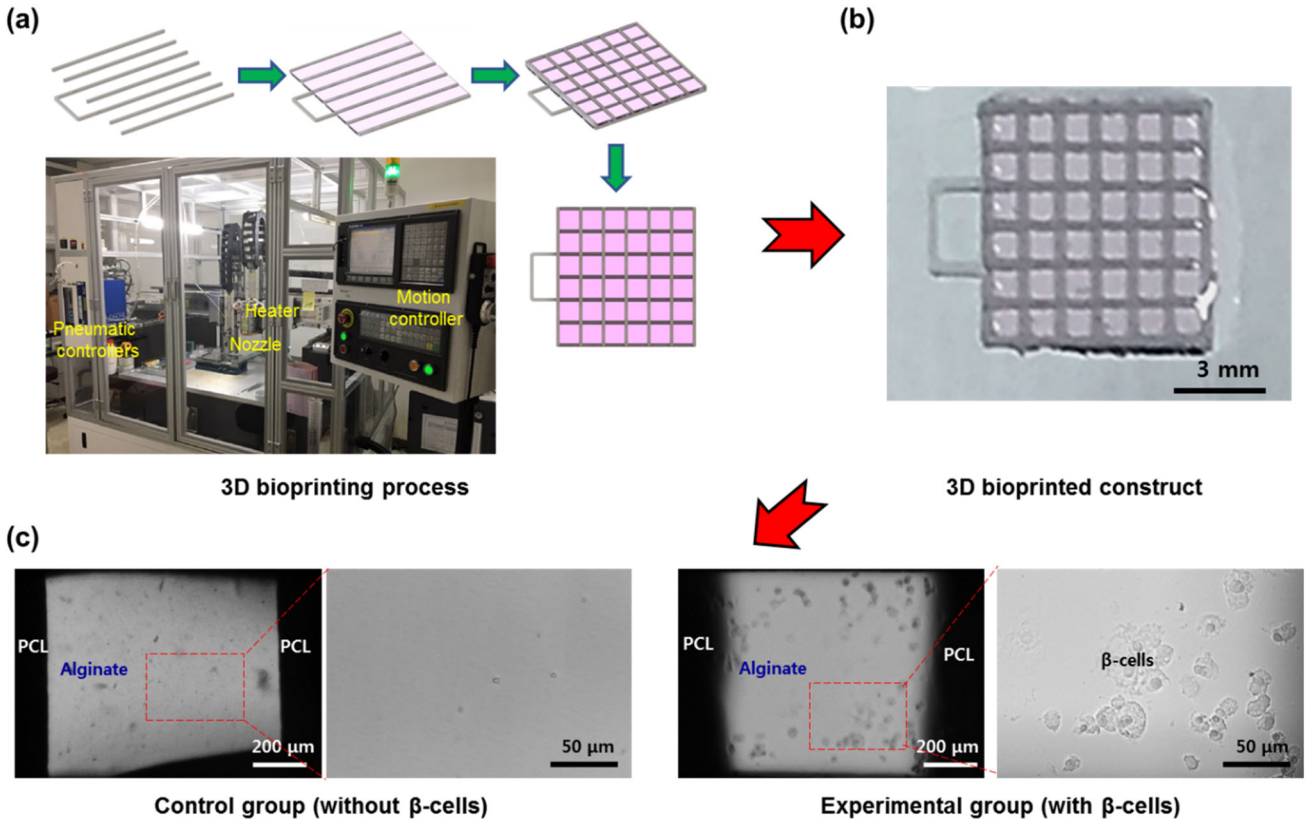

Fig. 1 Fabrication procedures for a β-cell (MIN-6)-laden, 3D-bioprinted construct. **a** Design and fabrication process for a 3D construct using a 3D-bioprinting system (center image). **b** Optical image of a β-cell (MIN-6)-laden, bioprinted construct. **c** Optical microscopic images of a β-cell loaded and unloaded alginate with a 3D-printed PCL frame

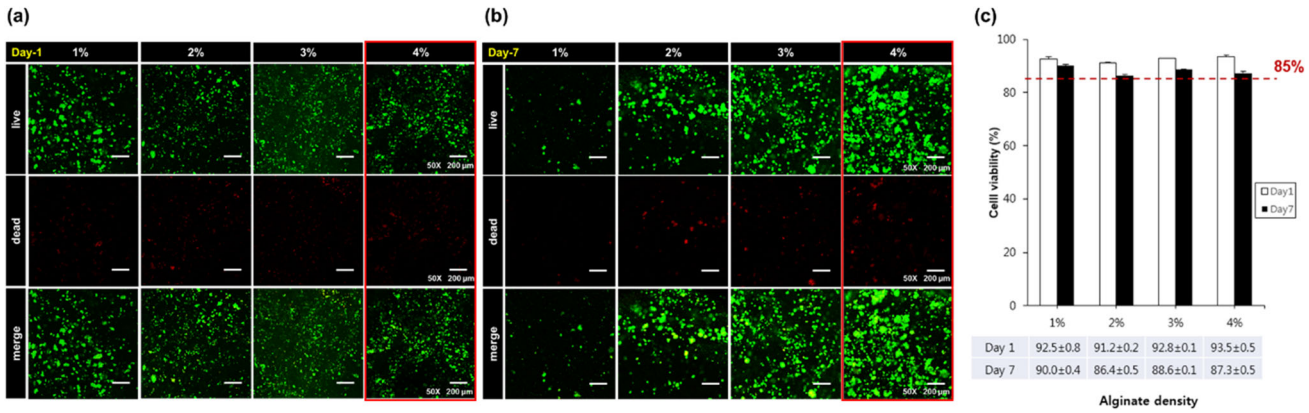

Fig. 2 Optimization of alginate density on the 3D-bioprinted, β-cell (MIN-6) construct. **a** Live/dead images of β-cells at various alginate densities (day 1). **b** Live/dead images of β-cells at various alginate densities (day 7). **c** Cell viability analysis results at various alginate densities. (Sample size: 10 mm (W) × 8 mm (D) × 0.6 mm (H), scale bar: 200 μm)

ELISA. As shown by the result of measuring insulin secretion from day 1 to day 28, it was increased by up to 2 times (215%) in the high-glucose state compared to the low-glucose state (Fig. 6). In other words, the developed, 3D-bioprinted construct secreted insulin in response to the amount of glucose injected.

Specifically, there was no significant increase from the beginning of construct construction to seven days. When compared to days 7, 14, and 21, insulin secretion increased by approximately 60% every 7 days as follows: 22 ± 1.39 (day 7), 36 ± 0.82 (day 14), and 48 ± 0.23 (day 21) under high-glucose conditions. Under low-glucose conditions, insulin

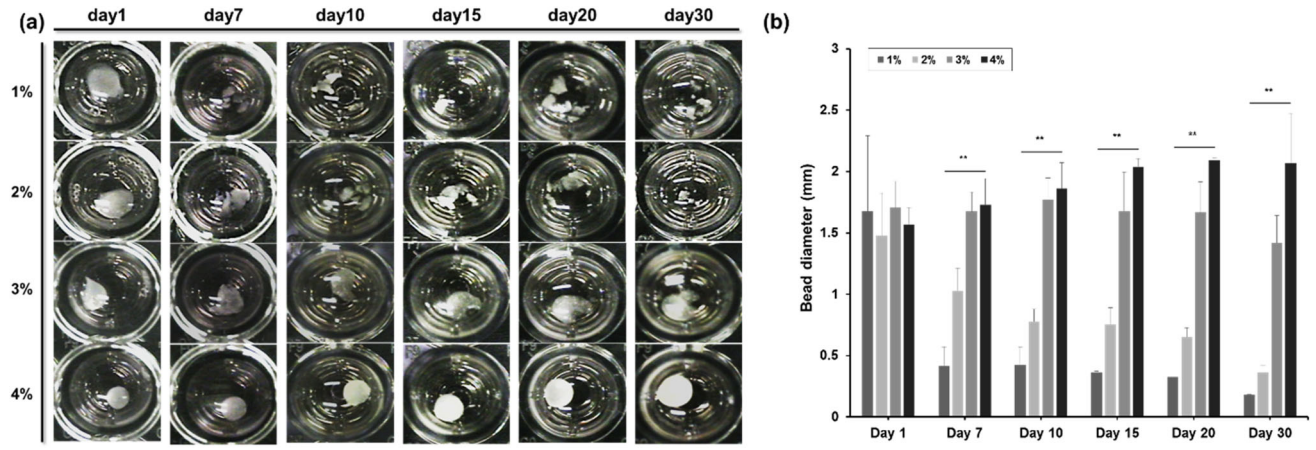

Fig. 3 Decomposition of alginate beads with various concentrations. **a** Optical images of changes of alginate beads during 30 days. **b** Comparison of bead diameter change according to alginate concentration. (**$P < 0.01$)

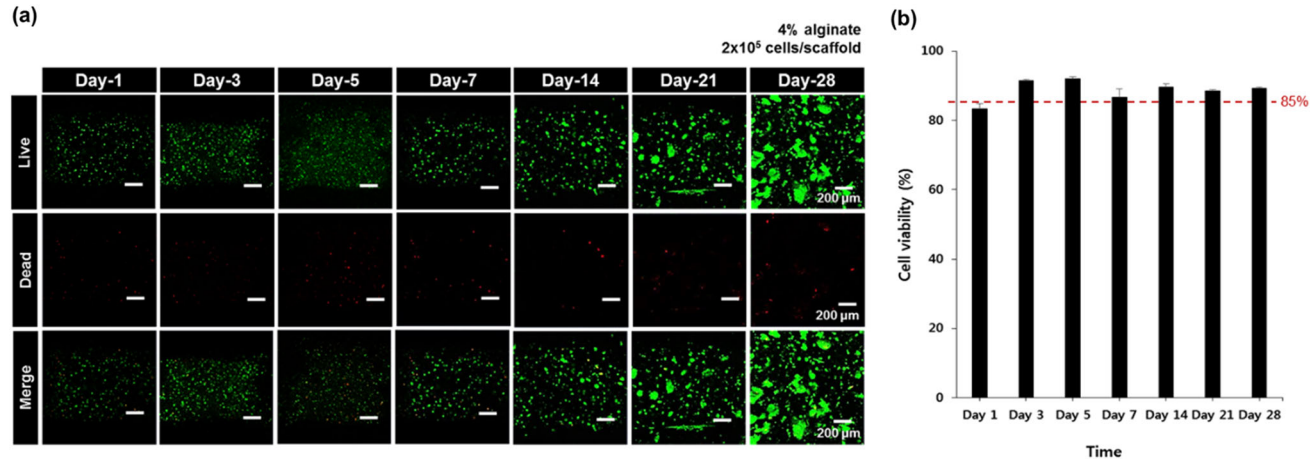

Fig. 4 β-Cell viability in the 3D-bioprinted construct. **a** Live/dead images of β-cells in the bioprinted constructs. **b** Cell viability analysis results for long-term, in vitro culture

secretion increased by 50 and 150% on day 14 (18 ± 1.03) and 21 (32 ± 1.74), respectively, compared to secretion on day 7 (13 ± 1.30). Insulin secretion was higher under high-glucose conditions than under low-glucose conditions at all time points (Supplementary Fig. S1). These results confirm that 3D-bioprinted MIN-6 cells maintained their insulin secretion ability even during long-term culture.

In vivo implantation results

Streptozotocin (STZ), a 2-deoxy-D-glucose derivative of 1-methyl-1-nitrosourea and similar in structure to glucose, is a drug that causes type 1 diabetes by inducing the death of pancreatic beta cells and preventing insulin secretion. In this study, a type 1 diabetic animal model was prepared by selecting mice with a blood glucose level of > 300 mg/dL among 8-week-old mice treated with STZ. Animal experiments were divided into control groups implanted with constructs without MIN-6 cells and experimental groups implanted with constructs containing MIN-6 cells. They were sacrificed at 28 and 56 days after implantation (Fig. 7a). In addition, once a week, glucose was measured from the mice for 56 days, and the change in the blood glucose level was analyzed (Fig. 7c).

Until day 21, there was no significant difference in blood glucose levels between the experimental groups (construct) and control groups. However, at days 42 and 56, the control group exhibited maximum blood glucose levels (> 600 mg/dL) in the measuring device, but the blood glucose levels of the experimental group implanted with the MIN-6 cell-laden scaffold decreased by ~ 11.2 and 7.2%, compared to the control group (600 mg/dL) (Fig. 7c).

When observing the transplanted samples after staining, a vascularization was not observed in either the control or experimental groups at 4 weeks. However, as shown in Fig. 8f, in the experimental group it was observed that the insulin was stained in the hydrogel structure printed with beta

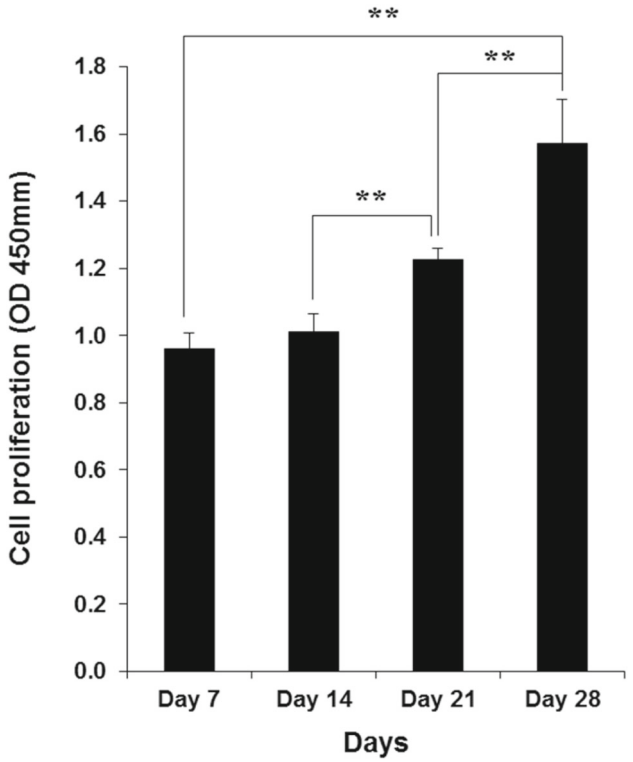

Fig. 5 Long-term proliferation results in the β-cell-laden, 3D-bioprinted construct. β-cells encapsulated in alginate by 3D bioprinting were proliferated for an extended period of 28 days (**P <0.01)

cells. Even after 8 weeks after transplantation, in the experimental group it was found that the insulin was stained by a brown color and over the entire area of the hydrogel printing (Fig. 8l). As shown in the H&E and CD31 staining results, in the experimental group (Figs. 8j and 8k), unlike in the control group (Figs. 8g and 8h), a number of blood vessels were observed at the inside and outside of the hydrogel-printed area.

Discussion

To date, various studies on pancreatic islets using 3D printing have been conducted. However, they had their drawbacks as they maintained a 2.5D structure and not a 3D structure and did not survive in vitro for a greater length of time [4, 27, 46]. To solve this problem, we developed a micro-environmental system for beta-cell culture using 3D-bioprinting technology and materials used in clinical settings. In particular, because hydrogels change rapidly in mechanical strength and cell survival rate, it is important to select an appropriate concentration. The selected concentration also significantly affects the 3D-bioprinting process [36, 39–41]. To date, various materials, such as matrigel, collagen, hyaluronic acid, and alginate, have been studied [4, 30–32]. Considering the supply and demand of materials, mechanical properties, and cell survival rate, 4 wt% of alginate was considered an optimal condition for the fabrication of the 3D-bioprinted construct.

In this study, we successfully fabricated a 3D-bioprinted construct using a combination of beta cells laden with 4% alginate and a PCL-constituting frame. In addition, to promote in vitro survival, the number of beta cells was increased, and a cluster of 100–200 μm was confirmed at 4 weeks. For islets, the clustering of beta cells is considered important for sustained survival and insulin secretion [27, 47–49]. Therefore, the 3D-bioprinted construct developed in this study can be considered a microenvironment suitable for beta-cell culture, long-term insulin secretion, and animal transplantation.

In the case of the hydrogel injection technique, performance cannot be maintained by the deviation of the beta cell

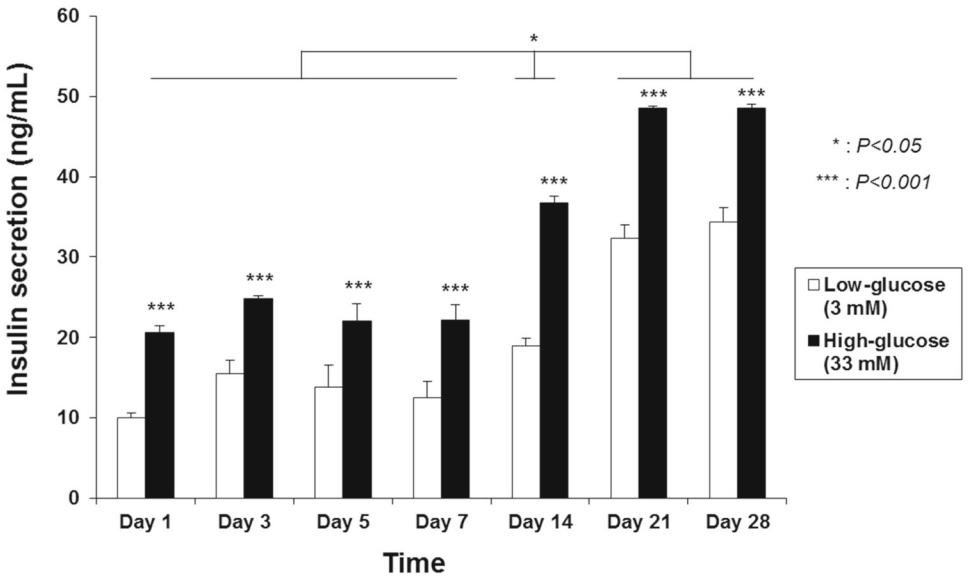

Fig. 6 Long-term insulin secretion levels of β-cell-laden, bioprinted constructs. In vitro cultured β-cells selectively reacted to the administration of high and low insulin concentrations for an extended period of 28 days (*P <0.05, ***P <0.001)

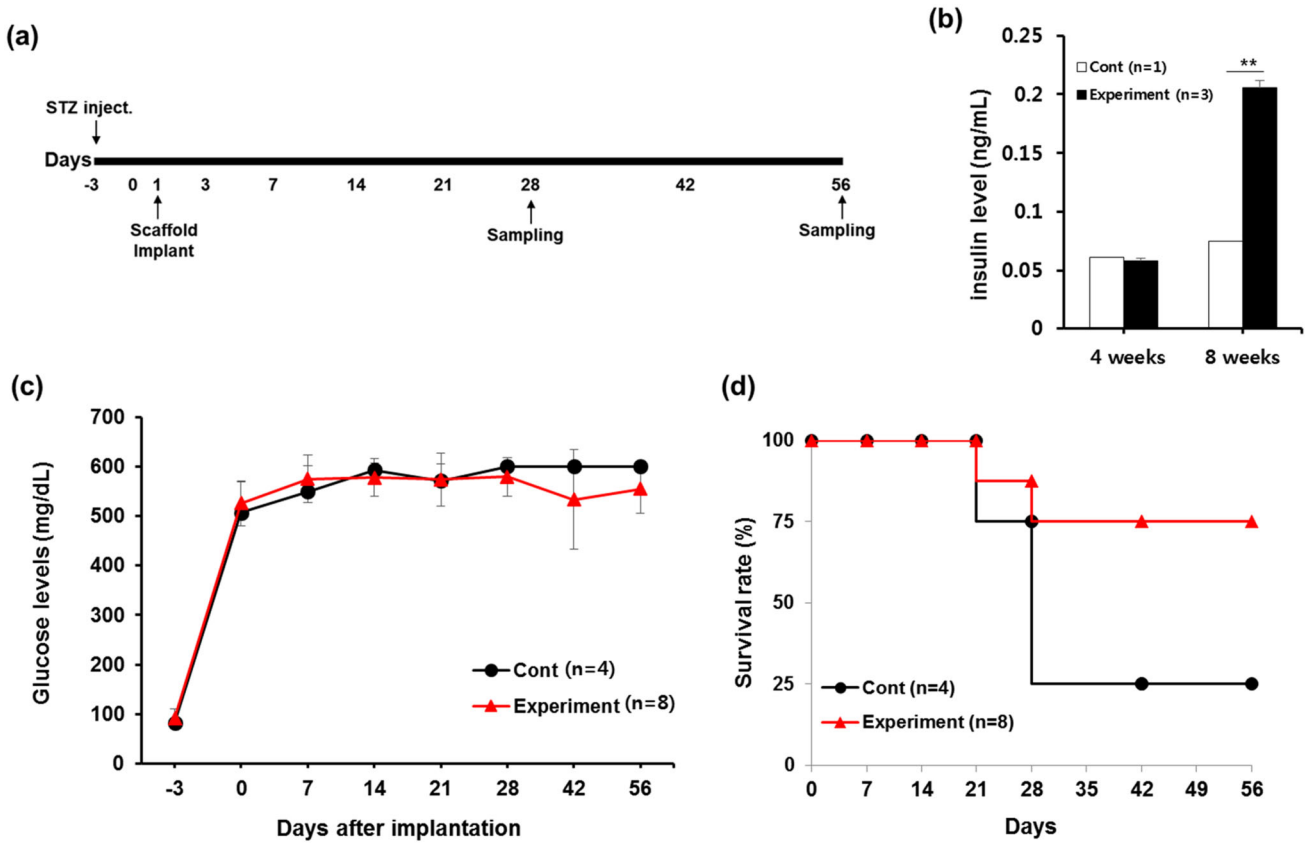

Fig. 7 Glucose/insulin levels in diabetic mice. **a** Experimental progress of the animal study using diabetic mice. **b** Results of measurements of insulin levels in diabetic mice with/without bioprinted constructs (**$P < 0.01$). **c** Measurement results of glucose levels in diabetic mice with/without bioprinted constructs. **d** Comparison of mice survival rates

from the normal position, and there is also a problem with cell engraftment to other organs [46]. Thus, 3D-bioprinted constructs that serve as scaffolds for cell adhesion and proliferation are necessary for the long-term survival of beta cells. In addition, a structure that can be implanted into the skin is more efficient than a portal vein procedure because of its lesser difficulty in terms of the surgical procedure [4].

The blood glucose levels in the control group (initially 300 mg/dL) continuously increased to exceed the maximum value of 600 mg/dL after 28 days, resulting in the death of three of the four experimental animals. In contrast, the blood glucose level in the experimental group (initially 300 mg/dL) increased only after two weeks. Further, as the transplanted beta cells functioned normally and secreted insulin, beta cells showed a decrease in blood glucose levels (min. 400 mg/dL) after two weeks.

Since the number of cells used in this experiment was not as large as a 2×10^5 cells/scaffold, reducing the blood glucose levels to normal was thought to present to be a challenge. It is thought this might be solved by additional 3D stacking of layers and an increase in the number of encapsulated beta cells.

When the developed 3D-bioprinted construct was transplanted into the subcutaneous layer of type 1 diabetic mice, the beta cells in the islets of Langerhans survived during the entire experimental period while maintaining insulin secretion (8 weeks). At week 4, there was a small difference in insulin secretion between the control and experimental groups. Insulin secretion in the latter at week 8 was three times higher than that in the former. This result was consistent with changes in the blood glucose levels (Fig. 7b). In other words, by releasing an appropriate amount of insulin after cell proliferation in the implanted, bioprinted construct, the blood glucose level in type 1 diabetic mice with STZ-induced pancreatic tissue damage was gradually decreased, as was the death rate, when compared with mice in control group. As shown in Fig. 7d, the survival rates of mice after 8 weeks of the experiment were 25% (control group) and 75% (experimental group), clearly indicating the performance and potential of the developed, 3D-bioprinted construct.

When the extracted graft material was stained after 4 weeks of animal experimentation, insulin was stained in the printed area in the experimental group in which the beta cells were bioprinted, but not in the control group (Figs. 8c

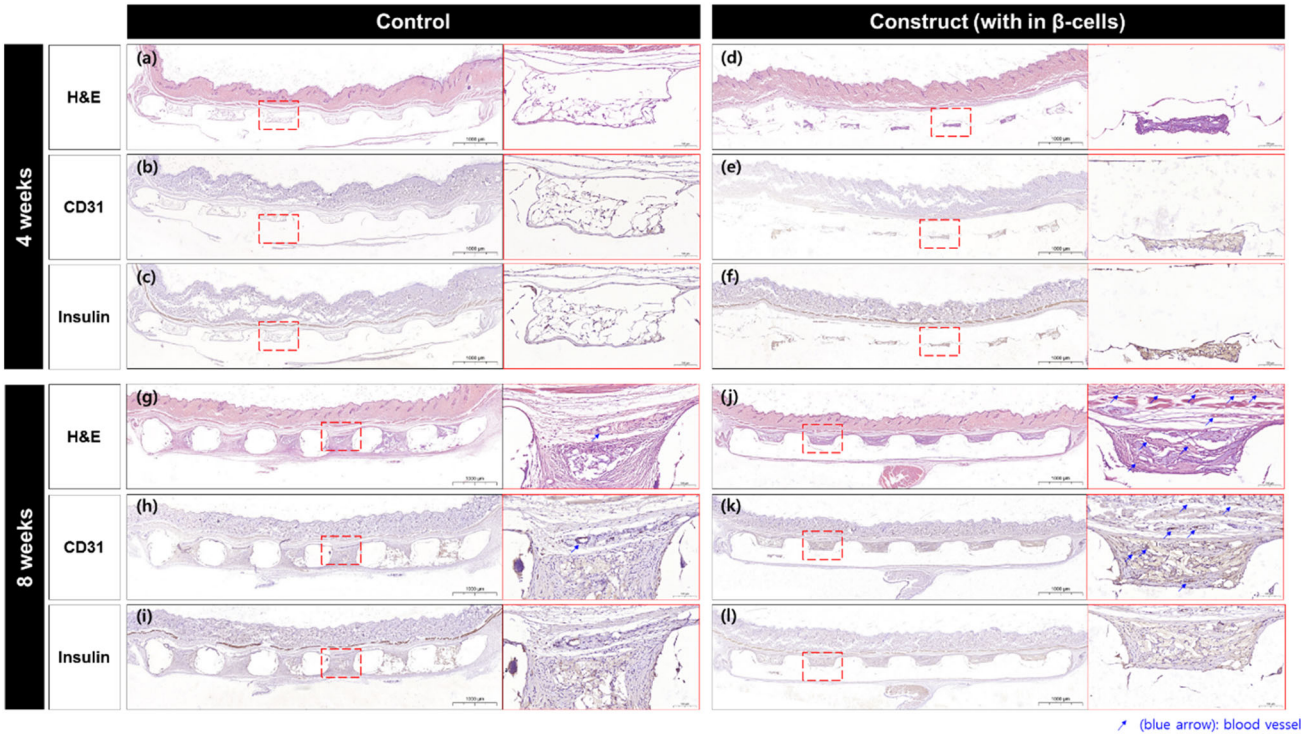

Fig. 8 Staining results of transplanted constructs. **a** H&E staining (control/4 weeks), **b** CD31 staining (control/4 weeks), **c** insulin staining (control/4 weeks), **d** H&E staining (construct/4 weeks), **e** CD31 staining (construct/4 weeks), **f** insulin staining (construct/4 weeks), **g** H&E staining (control/8 weeks), **h** CD31 staining (control/8 weeks), **i** insulin staining (control/8 weeks), **j** H&E staining (construct/8 weeks), **k** CD31 staining (construct/8 weeks), **l** insulin staining (construct/8 weeks) (blue arrow: blood vessel, brown color at **c**, **f**, **i**, **l**: stained insulin)

and 8f). In the sample, at week 8, a brown color was also clearly observed in the hydrogel printed in the experimental group (Figs. 8i and 8l). Also, when CD31 staining results and H&E staining results were observed at the same location of week 8 grafts, it was confirmed that a large number of blood vessels were generated around the bioprinted beta cells in the experimental group (Figs. 8j and 8k). That is, it was found that insulin secretion was progressed in the bioprinted tissue, and the insulin could be delivered into the mouse body through new blood vessels.

Collectively, these findings lead us to conclude that 3D-bioprinted beta cells may help improve blood glucose levels. If autologous beta cells using induced pluripotent stem cells, which have recently attracted research attention, are prepared, the developed beta-cell culture environment will be a technology with a high potential for type 1 diabetes treatment. Additionally, linking a host vessel to our construct could prove to be a more effective treatment.

Conclusions

In this study, we used 3D-bioprinting technology to fabricate a 3D construct that can maintain the function of beta cells for an extended time, and we proposed that transplanting the construct into the subcutaneous tissue rather than internal organs such as the portal veins can reduce the difficulty of transplantation and islet loss. The developed, 3D-bioprinted construct demonstrated rapid beta-cell proliferation for 4 weeks in vitro, and its laden beta cells were aggregated into a 100–200 μm diameter, similar to the original pancreatic islets. In addition, we confirmed that the construct faithfully fulfilled the function of beta cells by varying the amount of insulin secreted according to the amount of glucose. Subcutaneous transplantation experiments using type 1 diabetic mice with pancreatic islet destruction revealed that insulin secretion was normal for up to 8 weeks in the 3D-bioprinted construct. Blood glucose levels in mice continuously decreased during the 4-week experimental period. Although this study was conducted in mice using MIN-6, which is a mouse beta cell, the proposed strategy is suitable for clinical application in materials and 3D-bioprinting systems. Our results suggest that 3D-bioprinting technology can be a new option for the treatment of type 1 diabetes.

Supplementary Information The online version contains supplementary material available at https://doi.org/10.1007/s42242-021-00178-9.

Acknowledgements This research was supported by the Korea Health Industry Development Institute (KHIDI) funded by the Ministry of

Health & Welfare, Republic of Korea (No. HH21C0011), and Gachon University Gil Medical Center (No. FRD 2021-02).

Author contributions CBA, JHL, KHS, and JWL contributed to conceptualization; CBA and JHL were involved in validation; JHK, THK, and HSJ contributed to formal analysis; KHS and JWL were involved in writing—original draft, and project administration. All authors have read and agreed to the published version of the manuscript.

Declarations

Conflict of interest The authors declare that they have no conflict of interest.

Ethical approval The animal study protocol was approved by the Animal Subjects Committee of Gachon University (Approval number: LCDI-2018-0057). The institutional guidelines for the care and use of laboratory animals were followed.

Availability of data and materials Data are contained within the article.

References

1. Sneddon JB, Tang Q, Stock P et al (2018) Stem cell therapies for treating diabetes: progress and remaining challenges. Cell Stem Cell 22(6):810–823. https://doi.org/10.1016/j.stem.2018.05.016
2. Hu C, Jia W (2019) Therapeutic medications against diabetes: what we have and what we expect. Adv Drug Deliv Rev 139:3–15. https://doi.org/10.1016/j.addr.2018.11.008
3. IDF Diabetes Atlas (2017) International diabetes federation, 8th edn. Brussels, Belgium
4. Marchioli G, van Gurp L, van Krieken PP et al (2015) Fabrication of three-dimensional bioplotted hydrogel scaffolds for islets of Langerhans transplantation. Biofabrication 7:025009. https://doi.org/10.1088/1758-5090/7/2/025009
5. Graham ML, Schuurman H (2017) Pancreatic islet xenotransplantation. Drug Discov Today Dis Models 23:43–50. https://doi.org/10.1016/j.ddmod.2017.11.004
6. Bennet W, Sundberg B, Groth CG et al (1999) Incompatibility between human blood and isolated islets of Langerhans: a finding with implications for clinical intraportal islet transplantation? Diabetes 48(10):1907–1914. https://doi.org/10.2337/diabetes.48.10.1907
7. Paraskevas S, Maysinger D, Wang R et al (2000) Cell loss in isolated human islets occurs by apoptosis. Pancreas 20(3):270–276. https://doi.org/10.1097/00006676-200004000-00008
8. Thomas F, Wu J, Contreras JL et al (2001) A tripartite anoikis-like mechanism causes early isolated islet apoptosis. Surgery 130(2):333–338. https://doi.org/10.1067/msy.2001.116413
9. Thomas FT, Contreras JL, Bilbao G et al (1999) Anoikis, extracellular matrix, and apoptosis factors in isolated cell transplantation. Surgery 126(2):299–304. https://doi.org/10.1016/S0039-6060(99)70169-8
10. Lai Y, Schneider D, Kidszun A et al (2005) Vascular endothelial growth factor increases functional beta cell mass by improvement of angiogenesis of isolated human and murine pancreatic islets. Transplantation 79(11):1530–1536. https://doi.org/10.1097/01.tp.0000163506.40189.65
11. Pileggi A, Molano RD, Ricordi C et al (2006) Reversal of diabetes by pancreatic islet transplantation into a subcutaneous, neovascularized device. Transplantation 81(9):1318–1324. https://doi.org/10.1097/01.tp.0000203858.41105.88
12. Shapiro AM, Gallant HL, Hao EG et al (2005) The portal immunosuppressive storm: relevance to islet transplantation? Ther Drug Monit 27(1):35–37. https://doi.org/10.1097/00007691-200502000-00008
13. Billaudel B, Sutter BC (1982) Immediate in-vivo effect of corticosterone on glucose-induced insulin secretion in the rat. J Endocrinol 95(3):315–320. https://doi.org/10.1677/joe.0.0950315
14. Pagliuca FW, Millman JR, Gurtler M et al (2014) Generation of functional human pancreatic beta cells in vitro. Cell 159:428–439. https://doi.org/10.1016/j.cell.2014.09.040
15. Millman JR, Xie C, Van Dervort A et al (2016) Generation of stem cell-derived β-cells from patients with type 1 diabetes. Nat Commun 7:11463. https://doi.org/10.1038/ncomms11463
16. Hesse UJ, Sutherland DE, Gores PF et al (1986) Comparison of splenic and renal sub capsular islet autografting in dogs. Transplantation 41:271–274. https://doi.org/10.1097/00007890-198602000-00028
17. Kroon E, Martinson LA, Kadoya K et al (2008) Pancreatic endoderm derived from human embryonic stem cells generates glucose-responsive insulin secreting cells in vivo. Nat Biotechnol 26(4):443–495. https://doi.org/10.1038/nbt1393
18. Lacy PE, Hegre OD, Gerasimidi-Vazeou A et al (1991) Maintenance of normoglycemia in diabetic mice by subcutaneous xenografts of encapsulated islets. Science 254:1782–1784. https://doi.org/10.1126/science.1763328
19. Mridha AR, Dargaville TR, Dalton PD et al (2020) Prevascularized retrievable hybrid implant to enhance function of subcutaneous encapsulated islets. Tissue Eng A. https://doi.org/10.1089/ten.TEA.2020.0179
20. Motte E, Szepessy E, Suenens K et al (2014) Beta cell therapy consortium EU-FP7, composition and function of macro encapsulated human embryonic stem cell-derived implants: comparison with clinical human islet cell grafts. Am J Physiol Endocrinol Metab 307:E838–E846. https://doi.org/10.1152/ajpendo.00219.2014
21. Vegas AJ, Veiseh O, Gürtler M et al (2016) Long-term glycemic control using polymer-encapsulated human stem cell-derived beta cells in immune-competent mice. Nat Med 22(3):306–311. https://doi.org/10.1038/nm.4030
22. Veiseh O, Doloff JC, Ma M et al (2015) Size- and shape-dependent foreign body immune response to materials implanted in rodents and non-human primates. Nat Mater 14:643–651. https://doi.org/10.1038/nmat4290
23. Pedraza E, Brady AC, Fraker CA et al (2013) Macroporous three-dimensional PDMS scaffolds for extrahepatic islet transplantation. Cell Transpl 22:1123–1135. https://doi.org/10.3727/096368912X657440
24. Blomeier H, Zhang X, Rives C et al (2006) Polymer scaffolds as synthetic microenvironments for extrahepatic islets transplantation. Transplantation 82:452–459. https://doi.org/10.3727/096368912X657440
25. Dufour JM, Rajotte RV, Zimmerman M et al (2005) Development of an ectopic site for islet transplantation using biodegradable scaffolds. Tissue Eng 11:1323–1331. https://doi.org/10.1089/ten.2005.11.1323
26. Mao GH, Chen GA, Bai HY et al (2009) The reversal of hyper glycaemia in diabetic mice using PLGA scaffolds seeded with islet-like cells derived from human embryonic stem cells. Biomaterials 30(9):1706–1714. https://doi.org/10.1016/j.biomaterials.2008.12.030
27. Daoud JT, Petropavlovskaia MS, Patapas JM et al (2011) Long-term in vitro human pancreatic islet culture using three-dimensional micro fabricated scaffolds. Biomaterials 32(6):1536–1542. https://doi.org/10.1016/j.biomaterials.2010.10.036
28. Brady AC, Martino MM, Pedraza E et al (2013) Pro-angiogenic hydrogels within macroporous scaffolds enhances islet engraft-

ment in an extrahepatic site. Tissue Eng A 19:2544–2552. https://doi.org/10.1089/ten.TEA.2012.0686
29. Buitinga M, Truckenmüller R, Engelse MA et al (2013) Microwell scaffolds for the extrahepatic transplantation of islets of Langerhans. PLoS ONE 8:e64772. https://doi.org/10.1371/journal.pone.0064772
30. Mallett AG, Korbutt GS (2009) Alginate modification improves long-term survival and function of transplanted encapsulated islets. Tissue Eng A 15:1301–1309. https://doi.org/10.1089/ten.tea.2008.0118
31. De Vos P, De Haan BJ, Wolters GH et al (1997) Improved biocompatibility but limited graft survival after purification of alginate for microencapsulation of pancreatic islets. Diabetologia 40:262–270. https://doi.org/10.1007/s001250050673
32. Ludwig B, Reichel A, Steffen A et al (2013) Transplantation of human islets without immunosuppression. Proc Natl Acad Sci 110(47):19054–19058. https://doi.org/10.1073/pnas.1317561110
33. Ahn CB, Son KH, Yu YS et al (2019) Development of a flexible 3D printed scaffold with a cell-adhesive surface for artificial trachea. Biomed Mater 14:055001. https://doi.org/10.1088/1748-605X/ab2a6c
34. Ahn CB, Kim Y, Park SJ et al (2018) Development of arginine-glycine-aspartate-immobilized 3D printed poly(propylene fumarate) scaffolds for cartilage tissue engineering. J Biomater Sci Polym Ed 29:917–931. https://doi.org/10.1080/09205063.2017.1383020
35. Lee JW, Choi YJ, Yong WJ et al (2016) Development of a 3D cell printed construct considering angiogenesis for liver tissue engineering. Biofabrication 8:015007. https://doi.org/10.1088/1758-5090/8/1/015007
36. Lee JW, Soman P, Park JH et al (2016) A tubular biomaterial construct exhibiting a negative Poisson's ratio. PLoS ONE 11:e0155681. https://doi.org/10.1371/journal.pone.0155681
37. Lee JW, Kang KS, Lee SH et al (2011) Bone regeneration using a microstereolithography-produced customized poly(propylene fumarate)/diethyl fumarate photopolymer 3D scaffold incorporating BMP-2 loaded PLGA microspheres. Biomaterials 32:744–752. https://doi.org/10.1016/j.biomaterials.2010.09.035
38. Yu C, Ma X, Zhu W et al (2019) Scanningless and continuous 3D bioprinting of human tissues with decellularized extracellular matrix. Biomaterials 194:1–13. https://doi.org/10.1016/j.biomaterials.2018.12.009
39. You S, Wang P, Schimelman J et al (2019) High-fidelity 3D printing using flashing photopolymerization. Addit Manuf 30:100834. https://doi.org/10.1016/j.addma.2019.100834
40. Kang HW, Lee SJ, Ko IK et al (2016) A 3D bioprinting system to produce human-scale tissue constructs with structural integrity. Nat Biotech 34(3):312–319. https://doi.org/10.1038/nbt.3413
41. Koski S, Bose S (2019) Effects of amylose content on the mechanical properties of starch-hydroxyapatite 3D printed bone scaffolds. Addit Manuf 30:100817. https://doi.org/10.1016/j.addma.2019.100817
42. Ding H, Chang RC (2018) Simulating image-guided in situ bioprinting of a skin graft onto a phantom burn wound bed. Addit Manuf 22:708–719. https://doi.org/10.1016/j.addma.2018.06.022
43. Duin S, Schütz K, Ahlfeld T et al (2019) 3D bioprinting of functional islets of Langerhans in an alginate/methylcellulose hydrogel blend. Adv Healthc Mater 8(7):e1801631. https://doi.org/10.1002/adhm.201801631
44. Sun Y, Zhang M, Ji S et al (2015) Induction differentiation of rabbit adipose-derived stromal cells into insulin-producing cells in vitro. Mol Med Rep 12(5):6835–6840. https://doi.org/10.3892/mmr.2015.4305
45. Sun Y, Jiang BG, Li WT et al (2011) MicroRNA-15a positively regulates insulin synthesis by inhibiting uncoupling protein-2 expression. Diabetes Res Clin Pract 91(1):94–100. https://doi.org/10.1016/j.diabres.2010.11.006
46. Song J, Millman JR (2017) Economic 3D-printing approach for transplantation of human stem cell-derived β-like cells. Biofabrication 9:015002. https://doi.org/10.1088/1758-5090/9/1/015002
47. Nair GG, Liu JS, Russ HA et al (2019) Recapitulating endocrine cell clustering in culture promotes maturation of human stem-cell-derived β cells. Nat Cell Biol 21:263–274. https://doi.org/10.1038/s41556-018-0271-4
48. Seo H, Son J, Park JK (2020) Controlled 3D co-culture of beta cells and endothelial cells in a micro patterned collagen sheet for reproducible construction of an improved pancreatic pseudo-tissue. APL Bioeng 4:046103. https://doi.org/10.1063/5.0023873
49. Lin JY, Cheng J, Du YQ et al (2020) In vitro expansion of pancreatic islet clusters facilitated by hormones and chemicals. Cell Discov 6:20. https://doi.org/10.1038/s41421-020-0159-x